Measurement of Low-Energy Resonance Strengths in the $^{18}O(\alpha,\gamma)^{22}Ne$ Reaction

A. C. Dombos,[1,*] D. Robertson,[1,†] A. Simon,[1] T. Kadlecek,[2] M. Hanhardt,[2,3] J. Görres,[1] M. Couder,[1] R. Kelmar,[1] O. Olivas-Gomez,[1] E. Stech,[1] F. Strieder,[2] and M. Wiescher[1]

[1]*Department of Physics and The Joint Institute for Nuclear Astrophysics, University of Notre Dame, Notre Dame, Indiana 46556-5670, USA*

[2]*Department of Physics, South Dakota School of Mines and Technology, Rapid City, South Dakota 57701, USA*

[3]*South Dakota Science and Technology Authority, Sanford Underground Research Facility, Lead, South Dakota 57754, USA*

(Received 7 December 2021; revised 21 February 2022; accepted 31 March 2022; published 20 April 2022)

The $^{18}O(\alpha,\gamma)^{22}Ne$ reaction is an essential part of a reaction chain that produces the $^{22}Ne(\alpha,n)^{25}Mg$ neutron source for both the weak and main components of the slow neutron-capture process. At temperatures of stellar helium burning, the astrophysically relevant resonances in the $^{18}O(\alpha,\gamma)^{22}Ne$ reaction that dominate the reaction rate occur at α particle energies E_{lab} of 472 and 569 keV. However, previous experiments have shown the strengths of these two resonances to be very weak, and only upper limits or partial resonance strengths could be obtained. This Letter reports the first direct measurement of the total resonance strength for the 472- and 569-keV resonances, 0.26 ± 0.05 and 0.63 ± 0.30 μeV, respectively. New resonance strengths for the resonances at α particle energies of 662.1, 749.9, and 767.6 keV are also provided. These results were achieved in an experiment optimized for background suppression and detection efficiency. The experiment was performed at the Sanford Underground Research Facility, in the 4850-foot underground cavity dedicated to the Compact Accelerator System for Performing Astrophysical Research. The experimental end station used the γ-summing High EffiCiency TOtal absorption spectrometeR. Compared to previous works, the results decrease the stellar reaction rate by as much as $\approx 46^{+6}_{-11}$% in the relevant temperature range of stellar helium burning.

DOI: 10.1103/PhysRevLett.128.162701

In the field of nuclear astrophysics, the slow neutron-capture process, or *s* process, is the mechanism responsible for the abundance of roughly half of the stable nuclides beyond the iron peak that are observed in the solar system [1]. The two principal contributions to the *s* process are from the weak and main components, which produce $A < 90$ and $A = 90 - 205$ of the *s*-process abundance pattern, respectively, and occur in different astrophysical environments. The weak component occurs during core helium burning of massive stars. At the beginning of helium burning, ^{14}N remaining from the CNO cycles triggers the reaction chain $^{14}N(\alpha,\gamma)^{18}F(\beta^+\nu)^{18}O(\alpha,\gamma)^{22}Ne$. ^{22}Ne is gradually depleted by the $^{22}Ne(\alpha,\gamma)^{26}Mg$ reaction, but towards the end of helium burning the core contracts and eventually the temperature becomes high enough to trigger the $^{22}Ne(\alpha,n)^{25}Mg$ reaction with its negative Q value of -478.34 keV [2]. The main component occurs in thermally pulsing, low-mass asymptotic giant branch stars. Mixing occurs between protons from the outer envelope of the star and the intershell composed of helium and carbon. This mixing produces pockets of ^{13}C and ^{14}N within the intershell via $^{12}C(p,\gamma)^{13}N(\beta^+\nu)^{13}C(p,\gamma)^{14}N$. The ^{13}C pocket is then consumed by the $^{13}C(\alpha,n)^{16}O$ reaction, producing the majority of the neutron flux. Meanwhile, the ^{14}N pocket remains inactive until a thermal pulse occurs, initiating the sequence $^{14}N(\alpha,\gamma)^{18}F(\beta^+\nu)^{18}O(\alpha,\gamma)^{22}Ne$. A second neutron source is then available via the $^{22}Ne(\alpha,n)^{25}Mg$ reaction.

In both the weak and main *s*-process components, the $^{22}Ne(\alpha,n)^{25}Mg$ reaction plays an important role as a neutron source. The abundance of ^{22}Ne, and therefore the efficiency of $^{22}Ne(\alpha,n)^{25}Mg$ as a neutron source, during stellar helium burning relies on the preceding $^{18}O(\alpha,\gamma)^{22}Ne$ reaction rate. This reaction has been the subject of several experimental investigations [3–7] and a sensitivity study [8]. At temperatures of stellar helium burning ($T \approx 0.1 - 0.3$ GK), the astrophysically relevant resonances in the $^{18}O(\alpha,\gamma)^{22}Ne$ reaction occur at α particle energies of 472 and 569 keV [6]. These two resonances are extremely weak, and a measurement of the total resonance strengths has thus far remained elusive. Reference [5] was able to place upper limits of $< (0.0 \pm 0.2)$ and $< (2.0 \pm 0.5)$ μeV for the 472- and 569-keV resonances, respectively. An upper limit of ≤ 1.7 μeV was obtained for both resonances in Ref. [6]. The last attempt to measure these resonance strengths was reported in Ref. [7]. In that work, partial resonance strengths of 0.24 ± 0.08 and 0.63 ± 0.09 μeV were measured for the 472- and 569-keV resonances, respectively, by analyzing the γ-ray transition from the first excited state to the ground state in ^{22}Ne.

Assumptions were then made about γ-ray branching ratios to deduce total resonance strengths of 0.48 ± 0.16 μeV for the 472-keV resonance and 0.71 ± 0.17 μeV for the 569-keV resonance.

One challenge when measuring the yield from extremely weak resonances with traditional techniques is the low signal-to-background ratio. The main sources of background are beam-induced background from target impurities, natural radioactivity from the surrounding environment, and cosmic-ray induced background. In addition, these techniques may be hindered by incomplete information about γ-ray angular distributions and branching ratios. For these reasons, different approaches are being developed to study (α, γ) reactions. In this Letter, an environment that eliminates the main background sources was coupled with a total absorption spectrometer (thus removing the need for knowledge about γ-ray angular distributions and branching ratios), enabling the first direct measurement of the 472- and 569-keV total resonance strengths.

The experiment was performed at the Sanford Underground Research Facility (SURF) [9], in the 4850-foot underground cavity dedicated to the Compact Accelerator System for Performing Astrophysical Research (CASPAR) [10]. CASPAR consists of a 1 MV model JN electrostatic Van de Graaff accelerator, with a voltage range of approximately 150 kV–1.1 MV. The radio frequency (rf) ion source is capable of producing approximately 250 μA of protons and 220 μA of α particles. Ions are selected with a 25° analyzing magnet and sent to the experimental end station.

The experimental end station consisted of a target system surrounded by the High EffiCiency TOtal absorption spectrometeR (HECTOR) [11]. HECTOR is divided into 16 segments and has a 60 mm diameter borehole along the beam axis and provides a nearly 4π angular coverage for γ-ray detection. Each segment contains a NaI(Tl) crystal that is $4 \times 8 \times 8$ in. and surrounded by 1 mm of aluminium casing. Each segment is read out with two photomultiplier tubes (PMTs) and signals are recorded with the NSCL Digital Data Acquisition System (DDAS) [12].

The target system consisted of a tantalum pentoxide (Ta_2O_5) target mounted in a target holder, which was oriented 90° with respect to the beam direction. Multiple tantalum pentoxide targets were prepared by the anodic oxidation of 0.5 mm thick tantalum backings in water enriched to 97% in ^{18}O. This technique is proven to produce stable, uniform targets with a known stoichiometry and consistent thickness [13,14]. Because of the relatively high beam intensity for an extended period of time to maximize statistics, water cooling was applied to the backside of each target, and the stability and possible degradation of each target was monitored with the 334-keV resonance in $^{18}\mathrm{O}(p,\gamma)^{19}\mathrm{F}$ [15,16]. A scan of this resonance was performed for each target before and after usage. For all targets, the observed thickness obtained with the resonance scan before usage was within 10% of the expected value based on the anodizing voltage [13]. Though Ta_2O_5 targets are known to be very stable, an effort was made to not exceed 3 C of accumulated charge for each target to avoid any target degradation. Through the experiment the yields were monitored as a function of the total beam charge on target to ensure target stability. No significant degradation was observed for any target after beam irradiation.

The targets were anodized with 66 V (corresponding to a nominal thickness of 1056 Å of Ta_2O_5 and an energy loss of 56 keV at $E_\alpha = 677$ keV) and 200 V (corresponding to a nominal thickness of 3200 Å of Ta_2O_5 and an energy loss of 154 keV at $E_\alpha = 495$ keV).

A copper tube extended from the upstream direction to approximately 1 mm from the front of the target holder. The copper tube was cooled with liquid nitrogen to form a cold trap, which prevented the deposition of contaminants, such as hydrocarbons from the vacuum system, on the surface of the target. To suppress secondary electron emission from the target and obtain an accurate reading of the beam current on target, a bias voltage of -320 V was applied to the copper tube. The target system and beam pipe were electrically isolated from the rest of the beam line, and formed a Faraday cup to determine the integrated beam current on target.

The target system was installed at the end of the beam pipe, centered inside the borehole of HECTOR. In this configuration, the high geometric and intrinsic detection efficiency of HECTOR allows for resonance strengths to be measured with the γ-summing technique [11,17]. The ^{22}Ne nuclei produced from the $^{18}\mathrm{O}(\alpha,\gamma)^{22}\mathrm{Ne}$ reaction are formed in an excited state at an energy $E_{\mathrm{c.m.}} + Q$, where $E_{\mathrm{c.m.}}$ is the center-of-mass (c.m.) energy of the projectile-target system and Q is the reaction Q value (9666.82 keV [2]). Such excited states may de-excite through many different possible γ-ray cascades, but, with the γ-summing technique, the γ rays originating from the same cascade are summed together to create a sum peak at an energy $E_\Sigma = E_{\mathrm{c.m.}} + Q$ in the summed spectrum. Therefore, instead of analyzing individual γ rays from ^{22}Ne, only a single sum peak needs to be analyzed, and the number of sum-peak events is directly related to the number of (α,γ) reactions that took place, after taking into account the summing efficiency of HECTOR. The advantage of using the γ-summing technique with HECTOR at CASPAR is that the $^{18}\mathrm{O}(\alpha,\gamma)^{22}\mathrm{Ne}$ sum peaks are located in a region of the summed spectrum devoid of environmental and cosmic-ray background. In particular, the sum peaks for the weak 472- and 569-keV resonances could be identified with a relatively small amount of accumulated charge, which would be impossible for a similar setup in an above-ground environment.

The $^{18}\mathrm{O}(\alpha,\gamma)^{22}\mathrm{Ne}$ resonance strengths $\omega\gamma$ were calculated from

$$\omega\gamma = \frac{2}{\lambda_r^2}\varepsilon_r \frac{(N_\Sigma/\varepsilon_\Sigma)}{N_\alpha}, \tag{1}$$

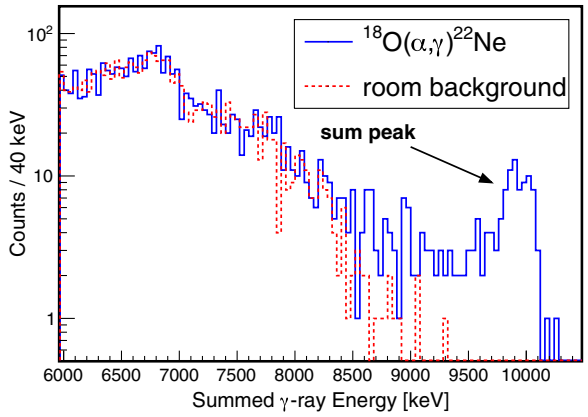

FIG. 1. Summed spectrum for an α beam impinging on a Ta_2O_5 target (anodized with 200 V) at $E_\alpha = 495.4$ keV after accumulating 3.96 C. Also plotted is the summed spectrum for normalized room background. The sum peak forms at an energy $E_\Sigma = E_{\text{c.m.}} + Q$, in a region of the summed spectrum devoid of background.

where λ_r^2 is the de Broglie wavelength in the c.m. frame, ε_r is the effective stopping power of the Ta_2O_5 target in the c.m. frame, N_Σ is the number of counts in the sum peak, ε_Σ is the summing efficiency of HECTOR, and N_α is the number of projectiles measured with the Faraday cup. SRIM-2013 [18,19] and the supplier-quoted number densities of the oxygen isotopes in the water were used to calculate ε_r.

The N_Σ and ε_Σ, were determined using the same analysis procedure as discussed in Ref. [11]. After obtaining the $^{18}O(\alpha,\gamma)^{22}Ne$ yield curve, statistics were collected at a beam energy on the resonance plateau for the thick-target yield ("on resonance") and at a beam energy slightly less than the resonance low-energy edge ("off resonance"). Figure 1 shows the on-resonance summed spectrum for the 472-keV resonance. After correcting for accumulated charge, the off-resonance spectrum was subtracted from the on-resonance spectrum. The resulting sum peak was then fitted with a Gaussian and linear background, following the procedure described in Ref. [11]. The linear background was subtracted and the resulting distribution was integrated in the region of three standard deviations below and above the sum-peak centroid to obtain N_Σ.

There are two methods for calculating the summing efficiency ε_Σ. In the statistical approach, ε_Σ depends on both the energy of the sum peak and the average γ-ray cascade multiplicity. The procedure to calculate ε_Σ as described in Ref. [11] relies on the segmentation of HECTOR and works on the principle that the average segment multiplicity is directly related to the average γ-ray cascade multiplicity. The average segment multiplicity is obtained from the "hit pattern," which is a distribution of the number of segments that detect energy in a sum-peak event. With GEANT4 [20] simulations, the relationship between average γ-ray cascade multiplicity, average segment multiplicity, and ε_Σ is known. The GEANT4 model of HECTOR at CASPAR has been verified by comparing experimental and simulated spectra for standard calibration sources such as ^{60}Co and ^{137}Cs, resonances from the $^{27}Al(p,\gamma)^{28}Si$ reaction [21], and resonances from the $^{18}O(\alpha,\gamma)^{22}Ne$ reaction.

The other method to calculate the summing efficiency uses the decay scheme of the resonance with GEANT4. In this approach, the summing efficiency is the ratio of the counts in the sum peak to the number of simulated events, provided the decay scheme is complete. The decay schemes of the 662.1-, 749.9-, and 767.6-keV resonances were verified based on a detailed analysis of the HECTOR spectra. Using the segmentation of HECTOR, the individual spectra of the 16 segments of HECTOR were created for only 662.1-, 749.9-, and 767.6-keV sum-peak events. These spectra are sensitive to the individual γ rays that participate in a γ-ray cascade. The corresponding hit patterns were also created. These experimental spectra were compared to simulated spectra using the primary γ-ray branching ratios in Table 3.2 of Ref. [22] and branching ratios for lower-lying levels from Ref. [23]. Excellent agreement was obtained in the comparison, indicating the decay schemes of these resonances are well known. While the decay schemes of the 662.1-, 749.9-, and 767.6-keV resonances are well known, no primary branching ratio information exists for the 472- and 569-keV resonances and therefore the statistical approach is the only available method for calculating ε_Σ for these two resonances.

Three sources of uncertainty contribute to the total uncertainty in the resonance strengths from the present Letter. There is the statistical uncertainty associated with the sum-peak integral, which was less than 4% for the 662.1-, 749.9-, and 767.6-keV resonances, but ≈17% for the 472-keV resonance and ≈47% for the 569-keV resonance. The uncertainty in the summing efficiency was determined using the approach described in Refs. [11,21] and was less than 5% for the 662.1-, 749.9-, and 767.6-keV resonances, but increased to ≈7% for the 472-keV resonance and ≈13% for the 569-keV resonance. Finally, a standard 5% uncertainty in the effective stopping power of the target was included for all resonances.

The resulting $^{18}O(\alpha,\gamma)^{22}Ne$ resonance strengths are listed in Table I. The resonance strengths calculated with summing efficiencies using the statistical approach and decay schemes are in agreement. The resonance strengths reported in this Letter are in a good agreement with those from previous measurements [4–6], and those used by Ref. [7] to calculate the previous stellar reaction rate except for the 472-keV resonance. The 472-keV resonance strength from the present Letter is less than the value from Ref. [7] and greater than the upper limit set by Ref. [5]. However, for the 472-keV resonance, there is good agreement between the partial resonance strength from Ref. [7] and the total resonance strength from the present Letter. In this case, the partial resonance strength obtained in Ref. [7]

TABLE I. Resonance parameters from Ref. [7] and this Letter for calculating the $^{18}O(\alpha,\gamma)^{22}Ne$ stellar reaction rate. The columns labeled "Statistical" and "Decay scheme" contain resonance strengths calculated with summing efficiencies using the statistical approach and decay schemes, respectively. See text for details.

		$\omega\gamma$ (μeV)		
			This Letter	
Energy (keV)	$\omega\gamma_{\text{partial}}$ (μeV) Ref. [7]	Ref. [7]	Statistical	Decay scheme
472 ± 18[a]	0.24 ± 0.08[c]	0.48 ± 0.16[c]	0.26 ± 0.05	
569 ± 15[a]	0.63 ± 0.09[c]	0.71 ± 0.17[c]	0.63 ± 0.30	
662.1 ± 1.0[b]		229 ± 19[c]	221 ± 12	225 ± 12
749.9 ± 1.0[b]		490 ± 40[c]	564 ± 35	553 ± 34
767.6 ± 1.0[b]		1200 ± 120[b]	1438 ± 86	1306 ± 77

[a]Calculated using the excitation energy in Table 3 of Ref. [6] and updated Q value of 9666.82 keV [2]. Reference [6] used a Q value of 9669.32 keV [24].
[b]Table II of Ref. [5].
[c]Table V of Ref. [7].

is most likely a total resonance strength, and the branching ratio to the ground state is smaller than originally assumed in that work.

The resonance energies of the low-energy resonances at $E_\alpha = 472$ and 569 keV could not be accurately determined from direct (α,γ) measurements, neither in the present Letter nor in previous experiments. However, the uncertainty in these resonance energies has a significant effect on the uncertainty in the stellar reaction rate. The α particle energies of 470 and 566 keV, given in, for example, Refs. [6,7], have been recalculated in the present Letter to be 472 and 569 keV, respectively, using the updated Q value of 9666.82 keV [2]. The original α particle energies of 470 and 566 keV were calculated using a Q value of 9669.32 keV [24]. Along with the updated Q value, the α particle energies were recalculated using only the excitation energies of ^{22}Ne from the $^{18}O(^6Li, d)^{22}Ne$ reaction [6]. The calculated α particle energies from this experiment are in good agreement with direct (α,γ) measurements at higher energies [4,5]. However, the α particle energies calculated from the excitation energies of ^{22}Ne from the $^{20}Ne(t,p)^{22}Ne$ reaction [25], which are used in some compilations [26–28], are not in good agreement, and therefore not used to recalculate the α particle energies in the present Letter. In any case, further experimental investigations are required to reduce the uncertainty in these resonance energies and hence the uncertainty in the stellar reaction rate.

Using the $^{18}O(\alpha,\gamma)^{22}Ne$ resonance strengths obtained in this Letter, we can calculate the stellar reaction rate solely using direct measurements of total resonance strengths. The result is shown in Fig. 2(a). The stellar reaction rate was calculated with the 472- and 569-keV resonance strengths obtained with the statistical summing efficiency, the 662.1-, 749.9-, and 767.6-keV resonance strengths obtained with the decay-scheme summing efficiency, and other resonance parameters from NACRE [29] (resonance energies from

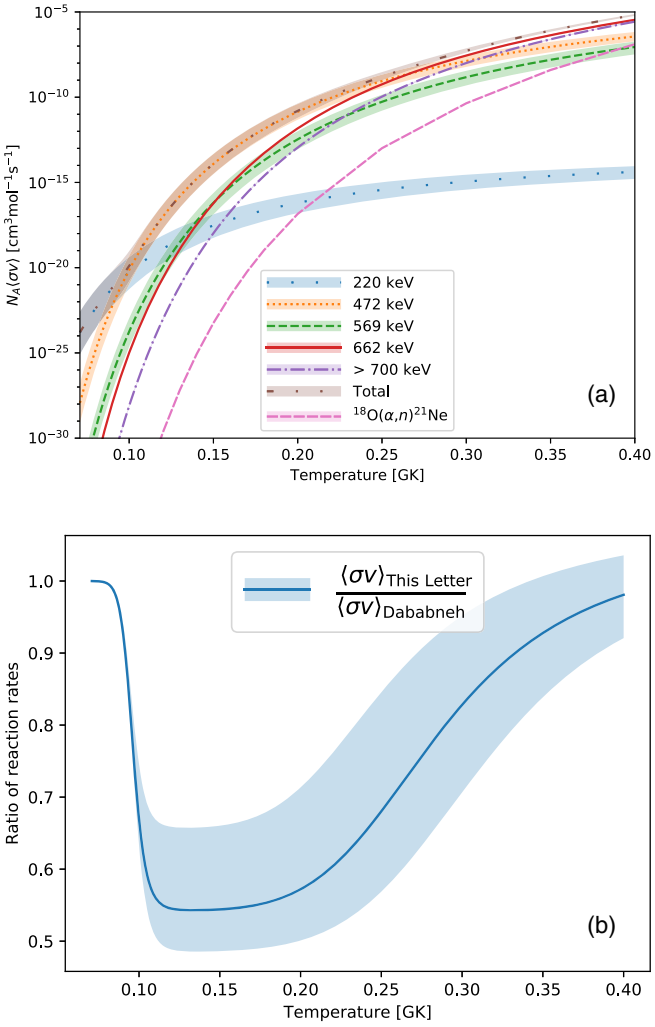

FIG. 2. The $^{18}O(\alpha,\gamma)^{22}Ne$ stellar reaction rate from this Letter (a) compared to the previous attempt [7] (b). The competing $^{18}O(\alpha,n)^{21}Ne$ rate [30] is insignificant.

NACRE have been recalculated using the updated Q value, as explained earlier in the text for the 472- and 569-keV resonances). At temperatures of stellar helium burning ($T \approx 0.1 - 0.3$ GK), the 472-keV resonance dominates the reaction rate, while at higher temperatures ($T > 0.3$ GK), the rate is dominated by the 662.1-keV and higher-energy resonances. Compared to Ref. [7], shown in Fig. 2(b), the rate decreases by as much as $\approx 46^{+6}_{-11}\%$ at $T \approx 0.13$ GK. In Ref. [7], one should note that the line labeled "$E_R > 700$ KeV" in the top panel of Fig. 11 is not reproduced by the rate as given by Eq. (6) of that paper. As shown in Fig. 2(a), the competing $^{18}O(\alpha, n)^{21}Ne$ rate [30] is insignificant compared to the $^{18}O(\alpha, \gamma)^{22}Ne$ rate.

In summary, we have performed the first direct measurement of the total resonance strength for the 472- and 569-keV resonances, and remeasured the 662.1-, 749.9-, and 767.6-keV resonance strengths in the $^{18}O(\alpha, \gamma)^{22}Ne$ reaction. The resonance strengths from this Letter decrease the stellar reaction rate by as much as $\approx 46^{+6}_{-11}\%$ in the relevant temperature range. Future work will investigate the impact this new rate has on the production of ^{22}Ne during stellar helium burning and hence the efficiency of ^{22}Ne as a neutron source for the weak and main s-process components.

This work was supported by the National Science Foundation (NSF) under Grants No. PHY-1713857, No. PHY-2011890, No. PHY-1614442, and No. PHY-1913746, and the Sanford Underground Research Facility (SURF) under Grant No. DE-SC0020216.

*adombos@nd.edu
†drobert4@nd.edu

[1] F. Käppeler, R. Gallino, S. Bisterzo, and W. Aoki, The s process: Nuclear physics, stellar models, and observations, Rev. Mod. Phys. **83**, 157 (2011).
[2] M. Wang, G. Audi, F. G. Kondev, W. J. Huang, S. Naimi, and X. Xu, The AME2016 atomic mass evaluation (II). Tables, graphs and references, Chin. Phys. C **41**, 030003 (2017).
[3] A. Adams, M. H. Shapiro, W. M. Denny, E. G. Adelberger, and C. A. Barnes, The $^{18}O(\alpha, \gamma)^{22}Ne$ reaction, Nucl. Phys. **A131**, 430 (1969).
[4] H. P. Trautvetter, M. Wiescher, K.-U. Kettner, C. Rolfs, and J. W. Hammer, Helium burning of ^{18}O, Nucl. Phys. **A297**, 489 (1978).
[5] R. B. Vogelaar, T. R. Wang, S. E. Kellogg, and R. W. Kavanagh, Low-energy reaction yields for $^{18}O(p, \gamma)$ and $^{18}O(\alpha, \gamma)$, Phys. Rev. C **42**, 753 (1990).
[6] U. Giesen, C. P. Browne, J. Görres, J. G. Ross, M. Wiescher, R. E. Azuma, J. D. King, J. B. Vise, and M. Buckby, The influence of low-energy resonances on the reaction rate of $^{18}O(\alpha, \gamma)^{22}Ne$, Nucl. Phys. **A567**, 146 (1994).
[7] S. Dababneh, M. Heil, F. Käppeler, J. Görres, M. Wiescher, R. Reifarth, and H. Leiste, Stellar He burning of ^{18}O: A measurement of low-energy resonances and their astrophysical implications, Phys. Rev. C **68**, 025801 (2003).
[8] F. Käppeler, M. Wiescher, U. Giesen, J. Görres, I. Baraffe, M. El Eid, C. Raiteri, M. Busso, R. Gallino, M. Limongi, and A. Chieffi, Reaction rates for $18O(\alpha, \gamma)22Ne$, $22Ne(\alpha, \gamma)26Mg$, and $22Ne(\alpha, n)25Mg$ in stellar helium burning and s-process nucleosynthesis in massive stars, Astrophys. J. **437**, 396 (1994).
[9] J. Heise, The Sanford underground research facility, J. Phys. Conf. Ser. **1342**, 012085 (2020).
[10] D. Robertson, M. Couder, U. Greife, F. Strieder, and M. Wiescher, Underground nuclear astrophysics studies with CASPAR, EPJ Web Conf. **109**, 09002 (2016).
[11] C. S. Reingold *et al.*, High efficiency total absorption spectrometer HECTOR for capture reaction measurements, Eur. Phys. J. A **55**, 77 (2019).
[12] C. J. Prokop, S. N. Liddick, B. L. Abromeit, A. T. Chemey, N. R. Larson, S. Suchyta, and J. R. Tompkins, Digital data acquisition system implementation at the National Superconducting Cyclotron Laboratory, Nucl. Instrum. Methods Phys. Res., Sect. A **741**, 163 (2014).
[13] D. Phillips and J. P. S. Pringle, Preparation of isotopic oxygen targets via the anodic oxidation of tantalum, Nucl. Instrum. Methods **135**, 389 (1976).
[14] A. Caciolli *et al.* (LUNA Collaboration), Preparation and characterisation of isotopically enriched Ta_2O_5 targets for nuclear astrophysics studies, Eur. Phys. J. A **48**, 144 (2012).
[15] M. Wiescher, H. W. Becker, J. Görres, K.-U. Kettner, H. P. Trautvetter, W. E. Kieser, C. Rolfs, R. E. Azuma, K. P. Jackson, and J. W. Hammer, Nuclear and astrophysical aspects of $^{18}O(p, \gamma)^{19}F$, Nucl. Phys. **A349**, 165 (1980).
[16] F. R. Pantaleo *et al.* (LUNA Collaboration), Low-energy resonances in the $^{18}O(p, \gamma)^{19}F$ reaction, Phys. Rev. C **104**, 025802 (2021).
[17] A. Simon *et al.*, SuN: Summing NaI(Tl) gamma-ray detector for capture reaction measurements, Nucl. Instrum. Methods Phys. Res., Sect. A **703**, 16 (2013).
[18] J. F. Ziegler, M. D. Ziegler, and J. P. Biersack, SRIM—The stopping and range of ions in matter (2010), Nucl. Instrum. Methods Phys. Res., Sect. B **268**, 1818 (2010).
[19] J. F. Ziegler, M. D. Ziegler, and J. P. Biersack, SRIM—The Stopping and Range of Ions in Matter, http://www.srim.org/.
[20] S. Agostinelli *et al.*, GEANT4—a simulation toolkit, Nucl. Instrum. Methods Phys. Res., Sect. A **506**, 250 (2003).
[21] O. Olivas-Gomez, A. Simon, D. Robertson, A. C. Dombos, F. Strieder, T. Kadlecek, M. Hanhardt, R. Kelmar, M. Couder, J. Görres, E. Stech, and M. Wiescher, Commissioning of the 4π γ-summing array HECTOR at CASPAR: Measurements of $^{27}Al(p, \gamma)^{28}Si$ resonances 4,850 feet underground, Eur. Phys. J. A **58**, 57 (2022).
[22] S. Dababneh, Alpha capture on ^{18}O during stellar He burning, Ph.D. thesis, 2002; Wissenschaftliche Berichte, FZKA-6782 (November 2002) Dissertation, Universität Heidelberg, 2002.
[23] M. Shamsuzzoha Basunia, Nuclear data sheets for A = 22, Nucl. Data Sheets **127**, 69 (2015).
[24] A. H. Wapstra and G. Audi, The 1983 atomic mass evaluation: (I). Atomic mass table, Nucl. Phys. **A432**, 1 (1985).
[25] Z. Q. Mao and H. T. Fortune, Mechanism of $^{20}Ne(t, p)$ and nuclear structure of ^{22}Ne, Phys. Rev. C **50**, 2116 (1994).
[26] P. M. Endt, Supplement to energy levels of $A = 21 - 44$ nuclei (VII), Nucl. Phys. **A633**, 1 (1998).

[27] C. Iliadis, R. Longland, A. E. Champagne, A. Coc, and R. Fitzgerald, Charged-particle thermonuclear reaction rates: II. Tables and graphs of reaction rates and probability density functions, Nucl. Phys. **A841**, 31 (2010).

[28] C. Iliadis, R. Longland, A. E. Champagne, and A. Coc, Charged-particle thermonuclear reaction rates: III. Nuclear physics input, Nucl. Phys. **A841**, 251 (2010).

[29] C. Angulo *et al.*, A compilation of charged-particle induced thermonuclear reaction rates, Nucl. Phys. **A656**, 3 (1999).

[30] A. Best, S. Falahat, J. Görres, M. Couder, R. deBoer, R. T. Güray, A. Kontos, K.-L. Kratz, P. J. LeBlanc, Q. Li, S. O'Brien, N. Özkan, K. Sonnabend, R. Talwar, E. Uberseder, and M. Wiescher, Measurement of the reaction $^{18}\mathrm{O}(\alpha, n)^{21}\mathrm{Ne}$, Phys. Rev. C **87**, 045806 (2013).